16. Rehabilitation of a Low-Head Gravitational Vortex Site with an Improved Vortex Turbine

In many countries all over the world, a significant part of hydropower has not been developed due to the head limitations and design constraints of traditional turbines. The complexity with these low head sites is the large flow required to reach sizable power production. When trying to utilize classic turbine designs for these sites, debris, cavitation, and an uneconomical scaling of the rotor hinder a successful business case. Therefore, new turbines are emerging on the market, like the vortex turbine and water wheels [10,71]. These machines allow the exploitation of low head sites at low cost and using civil works constructed with local labor when using a new non-conventional turbine. Among new low head hydropower converters, the novel vortex turbine [10] has been developed and installed in several installations all over the world. Previous Gravitational vortex turbine designs have shown the usefulness of the technology, but the rotor and basin dimensions were such that the solution reached a higher cost per kW. The current vortex turbine design, as proposed by Turbulent, was designed to solve these issues and make the vortex technology a realistic option for hydropower development of these low head sites in small and mid-sized rivers and increase the use of vortex turbines for rural electrification. Depending on model size, the Turbulent vortex turbine can operate within a head range of 1–4.5 m and a flow range of 0.7–9 m^3/s.

The current case study describes the replacement of the rotor, drivetrain, and power electronics of a previously installed gravitational vortex turbine in Bali. This turbine is installed to provide sustainable energy to the Green School by using the small head difference and large flow of the Ayung River. The site has a head of 1.85 m and a flow of 1.5 m^3/s. The previous turbine was not able to produce more than 5 kW in practice, possibly due to technical problems with the generator. The rotor also required a large amount of maintenance as it would get blocked by debris (coconuts, branches, palm fronts and stones) which are abundant in the Ayung river. After a flood destroyed the drivetrain and power electronics a new solution was needed.

16.1. Design Parameters

Based on the site head and flow, a turbine diameter of 1.18 m was calculated, which corresponds to a required basin diameter of 3.9 m. The outlet is usually designed to be free (discharging to atmospheric pressure) or can be equipped with a diffuser (negative pressure at the outlet). However, for this site, the existing basin has a diameter of 7.9 m. The outlet is submerged by about 15–20 cm (Figure 56c), that would lead to Carnot shock losses [72], and the construction of a diffuser was not feasible due to site constraints.

(a) (b) (c)

Figure 56. (a) Turbulent vortex turbine concept; (b) previous vortex turbine and (c) submerged outlet at nominal flow.

These factors necessitated a customized solution for the retrofit so that the performance measures are acceptable even for the oversized basin. A series offree-surface CFD simulations were conducted using the interFoam solver in OpenFOAM (Figure 57) to size the rotor and validate the performance of the retrofit. After commissioning, it was found that the measured performance of the plant slightly exceeds performance predicted by CFD, possibly due to some uncertainty in outlet tailwater level measurements. The turbine size and performance measures are listed in Table 11.

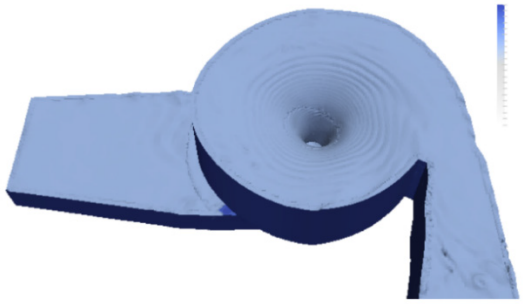

Figure 57. Computational Fluid Dynamics (CFD) model for Bali turbine.

Table 11. Turbine size and performance metrics.

Parameter	Value
Impeller diameter	1.18 m
Blade row height	0.44 m
Speed	96 rpm
Nominal flow	1.5 m^3/s
Predicted head	2.05 m
Measured	1.85 m
Net predicted power	14.1 kW
Net Measured power	13 kW
Predicted hydr. e ffi ciency	54.6%
Measured hydr. e ffi ciency	55.8%

This optimization allows the Turbulent design to produce 13 kW with the current site. Due to the design of the Turbulent turbine, this could be achieved with a relatively small and lightweight turbine (rotor and drive train are approximately 6 times smaller than the previous gravitational vortex turbine and weight is limited to 550 kg) and at a relatively low cost (0.07 EUR /kWh incl. maintenance).

The turbine itself was installed in less than one day (Figure 58), commissioning was completed after three days. The flood-proof design was tested just one day after installation during an evening storm (Figure 59). The turbine not only survived the flood but also let all the debris and bed load pass through without harm to the blades or structure.

Figure 58. Installation with winch (left) and manual lifting (right) first test run.

Figure 59. First flood event with inlet completely submerged.

16.2. Low Ecological Impact

The design of a vortex turbine allows it to be installed in rivers with minimal head di fferences. In the case of this site in Bali, the head was already available due to a natural cascade of boulders. To ensure enough water would deviate into the turbine, a small gabion weir (2.5 m width, 1.5 m height) was built (Figure 60, left side). A 20-meter bypass canal brings the water to the turbine after which it is returned straight back into the river. This way the river flow is not interrupted and no barrier for fish movement is created.

Figure 60. Intake structure.

16.2.1. Ecologically Improved Design

Fish friendly turbines are becoming more and more important, especially under the EU water framework. With that in mind, the turbine was designed according to criteria from previous research on turbine fish-friendliness by Amaral et al. [73], Cada et al. [74] and Cook et al. [75]. Potential damage mechanisms are identified in four categories: mechanical injury (strike, grinding, etc.), pressure (exposure to decreased pressure and rate of pressure decrease), shear /turbulence and cavitation [74]. Out of these, mechanical injury mechanisms are considered dominant, and among these, a leading-edge blade strike is assumed likely to be the primary cause of fish mortality due to turbine passage in many hydropower plants [73]. Physoclistous fishes are very susceptible to injury /mortality due to sudden pressure decrease that leads to swim bladder rupture or internal hemorrhaging [76]. In this study, the considered turbine is evaluated against thresholds for leading-edge strike, barotrauma and shear flow-related injury, using steady-state MRF (multiple-rotating frame) CFD simulations.

16.2.2. Leading Edge Strike

Amaral et al. [73] conducted two-species experiments with di fferent fish lengths (L) and blade thicknesses (t), and found that there was little or no fish mortality (97–100% total survival rate) for blade strike speeds (relative velocity between fish and blade) up to 5 m /s. Figure 61a reproduced from that study [73] shows the data points and linear regression relations between total survival percentage and strike speed for varying L/t ratios. In Figure 61b, the relative velocities for the studied vortex turbine are plotted. The relative velocities are almost entirely below the 5 m /s threshold throughout the flow passage area, except very tiny portions at boundary layers shown in grey. Following the reasoning by Cook et al. [75], such tiny non-compliant volumes minimize damages to fish.

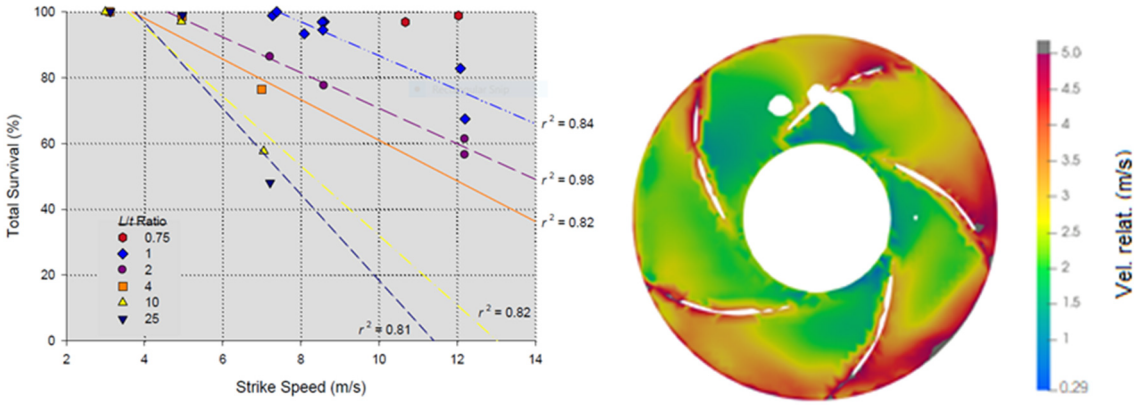

(a) (b)

Figure 61. (a) Total survival vs. strike speed for di fferent L/t ratios; (b) relative velocity (m /s) at leading edge ((a) reproduced with permission from authors).

16.2.3. Pressure Decrease

Based on a review of past studies, Cada et al. [74] found that when the pressure drop is less than 40% of the fish acclimation pressure (i.e., the pressure ratio > 60%), then there is little or no fish-mortality. Between 1973–1986, the water level was measured to be 0.55–0.88 m in the Ayung river [77]. The maximum acclimation depth of fishes in the Ayung river was conservatively assumed to be twice the maximum depth (1.76 m) in the absence of more specific data. The equivalent maximum acclimation pressure, P_a = 17.19 psa. From Figure 62, the minimum exposure pressure, $P_e = -1.1 \times 10^4$ P_a (relative) = 13.1 psa. Thus, the ratio P_e/P_a = 76%, which is safely above the threshold limit (60%).

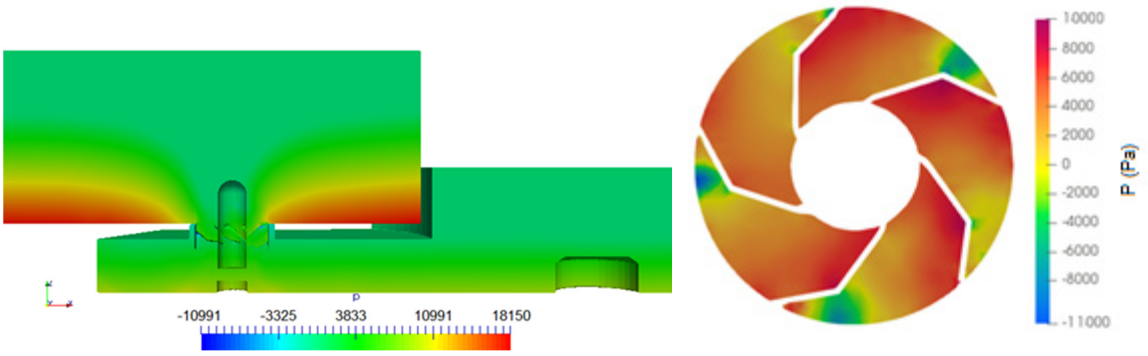

Figure 62. Pressure plot shown on a longitudinal section, and Pressure plotted on cross-section.

16.2.4. Rate of Pressure Decrease

Based on the experimental results by Abernethy et al. [76], Cook et al. established −500 psi/sec as the fish-friendly threshold of pressure decrease rate for Alden turbine design criterion [75]. In this study, we follow the same criterion and compare the actual pressure drop rate with this value. While there is some uncertainty regarding fish behavior during runner passage, previous studies have assumed fishes to follow flow streamlines like mass-less particles (e.g., Richmond et al. [78]). Under this assumption, the rate of pressure decrease (as experienced by a fish as it travels through the turbine) can be calculated using the material derivative of pressure that contains an advection part and an unsteady part:

$$\frac{Dp}{Dt} = \frac{\partial p}{\partial t}(\text{unsteady}) + V \cdot (p) = 0 + V_r \cdot {}_r(p) = V_r \cdot R(\theta) (p) \quad (2)$$

where $\frac{Dp}{Dt}$ is the material derivative of pressure, $\frac{\partial p}{\partial t}$ is the transient (unsteady) part, V, (p) and V_r, ${}_r(p)$ are fluid velocities and pressure gradients in stationary and rotating coordinate frames respectively, $R(\theta)$ is the rotation matrix with θ being the angle between the two frames. In a steady state MRF CFD simulation, the rotating coordinate frame instantaneously coincides with the CFD coordinate system, $(p) = {}_r(p)$. Thus, $\frac{Dp}{Dt} = V_r \cdot (p)$. The RHS is evaluated in CFD and plotted in Figure 63a (longitudinal section) and Figure 63b (cross-section at mid-height ofimpeller). Throughout the flow area, except at localized hotspots, the pressure drop rates are very gradual. The maximum pressure drop rate is less than 116 psi /s and safely lower than the threshold limit of 500 psi /s.

16.2.5. Shear Strain Rate

Based on previous studies, the fish-friendly threshold for the shear strain rate was taken as 500 s^{-1} (Cook et al. [75]). The fluid strain rates in XY, YZ and ZX planes are plotted in Figure 64a–c, respectively. The strain rates are safety limited below the safety threshold except very tiny areas shown in grey, which can be deemed inconsequential (Cook et al. [75]).

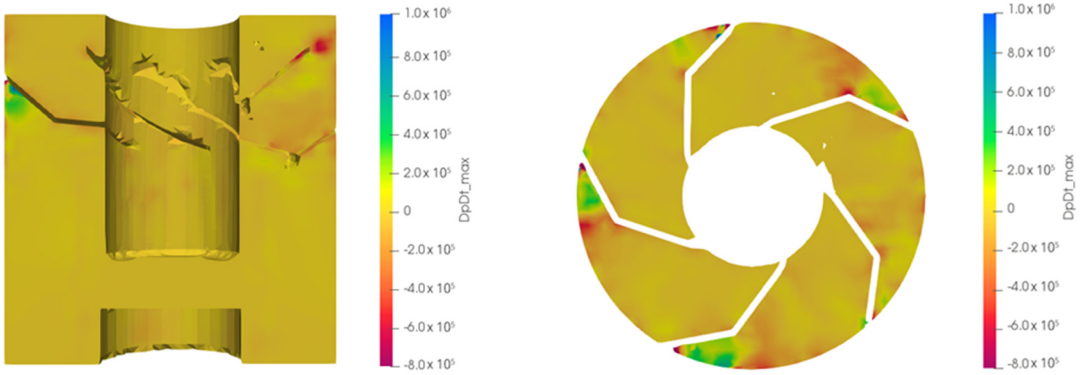

(a) (b)

Figure 63. Dp/Dt over ZX plane (vertical section, on the left (a)), Dp /Dt over XY plane (cross-section, right (b)).

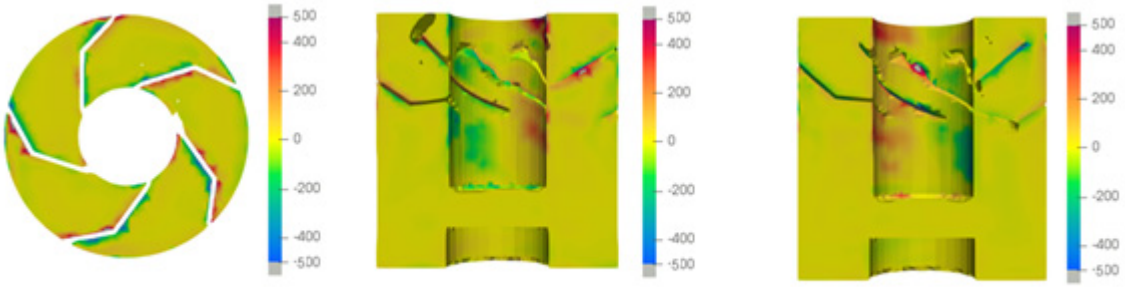

(a) XY strain rate (s^{-1}) (b) YZ strain rate (s^{-1}) (c) ZX strain rate (s^{-1})

Figure 64. Strain rates along di fferent planes, (a) XY, (b) YZ, (c) ZX.

16.3. Conclusions

The novel Turbulent vortex turbine design, combined with the refurbishment of the existing gravitational vortex basin structure, can be seen as a successful case that demonstrates that a vortex turbine can produce energy at an acceptable cost while also minimizing ecological impact. The current study indicates the fish-friendliness of the turbine based on CFD results and established fish-friendliness metrics. However, detailed on-site testing will be conducted in the near future to better investigate this aspect, which is a complex problem depending also on fish behavior.